Evolution and termination of H-modes in NSTX

2002 Plasma Phys. Control. Fusion 44 A323

(http://iopscience.iop.org/0741-3335/44/5A/334)

INSTITUTE OF PHYSICS PUBLISHING PLASMA PHYSICS AND CONTROLLED FUSION

Plasma Phys. Control. Fusion **44** (2002) A323–A332 PII: S0741-3335(02)34500-7

Evolution and termination of H-modes in NSTX

C E Bush[1], R Maingi[1], M G Bell[2], R E Bell[2], E D Fredrickson[2], D A Gates[2], S M Kaye[2], S Kubota[3], H W Kugel[2], B P LeBlanc[2], R Maqueda[4], S Medley[2], J E Menard[2], D Mueller[2], F Paoletti[5], S Paul[2], S A Sabbagh[5], V A Soukhanovskii[2], D Stutman[6], G Taylor[2], S J Zweben[2], D W Johnson[2], R Kaita[2], M Ono[2], Y-K M Peng[1], A L Roquemore[2] and E J Synakowski[2]

[1] Oak Ridge National Laboratory, Oak Ridge, TN 37831, USA
[2] Princeton Plasma Physics Laboratory, PO Box 451, Princeton, NJ 08543, USA
[3] University of California at Los Angeles, Los Angeles, CA 90095, USA
[4] Los Alamos National Laboratory, Los Alamos, NM 87545, USA
[5] Columbia University, New York, NY, USA
[6] Johns Hopkins University, Baltimore, MD 87545, USA

Received 5 September 2001
Published 29 April 2002
Online at stacks.iop.org/PPCF/44/A323

Abstract

The dynamic evolution of the first National Spherical Torus Experiment (NSTX) H-modes will be discussed. The H-modes were obtained in lower-single null divertor discharges with various forms of plasma heating. The exact timing of divertor formation and also the NBI power level affects both whether or not the discharge exhibits ELMs and the duration of the ELM-free phase. ELM-free discharges had energy confinement as high as 120 ms, whereas the few discharges with ELMs had confinement times ∼50–70 ms. Buildup of a steep edge density gradient and formation of 'ears' on the density profile were observed within a few ms of the L–H transition, yielding broader density and pressure profiles. The L–H transition was marked by a decrease in edge visible light and simultaneous increase in electron Bernstein wave emission, reflecting a steepening of the edge density gradient. Gas puff imaging of He-I light during the H-mode phase showed rapid formation of a narrow emission layer ∼2 cm wide in the H-mode phase, which returned within 20 microseconds at termination of the H-mode phase to a broader turbulent emission layer. All of the H-modes were terminated by an MHD reconnection event. The first power threshold (P_{th}) study showed the neutral beam injection power (P_b) component of P_{th} to be $\leqslant 0.84$ MW, higher than that predicted by the ITER database scaling.

1. Introduction

H-modes with high stored energy and strong edge density gradients have been obtained on National Spherical Torus Experiment (NSTX) with good reproducibility. Significant

experience, progress and extension of the H-mode operating space has been gained since earlier reports on the NSTX H-mode [1, 2]. L- to H-transitions have occurred using neutral beam injection (NBI) heating only, RF heating only (high harmonic fast wave (HHFW)) and RF + NBI. NSTX is a spherical torus (ST) capable of producing a plasma of nominal parameters: $R = 0.85\,\mathrm{m}$, $a = 0.67\,\mathrm{m}$, $0.3 < I_\mathrm{p} \leqslant 1.4\,\mathrm{MA}$ for NBI heated plasmas, $B_\mathrm{t} \leqslant 0.6\,\mathrm{T}$, $\kappa \leqslant 2.3$, $\delta \leqslant 0.5$ and $\mathrm{n_e} = (1\text{–}7) \times 10^{19}\,\mathrm{m^{-3}}$, where I_p = plasma toroidal current, B_t = toroidal magnetic field, κ = elongation, δ = triangularity and $\mathrm{n_e}$ = line-average density. The present heating capability includes 5 MW of NBI and 6 MW of HHFW heating. Elongations of 1.6–2.3 have been achieved. The largest STs are NSTX ($R/a = 0.85\,\mathrm{m}/0.67\,\mathrm{m}$, aspect ratio $R/a \geqslant 1.27$) at PPPL and mega-ampere spherical tokomak (MAST) [3]; $R/a = 0.85\,\mathrm{m}/0.65\,\mathrm{m}$, aspect ratio = 1.31) located at the Culham Science Center in England.

Studies are underway to understand the dynamic evolution and termination of the NSTX H-modes in order to be able to create them reproducibly, to control them and to utilize them to achieve the high β_t and performance goals of the NSTX program [4, 5]. ELM-free and ELMy H-modes have been obtained with NBI and/or RF heating [6]. The edge transport barrier is evident by 'ear' shaped peaks on the edge density profile, which develop and remain for the duration of ELM-free H-modes. Electron Bernstein wave (EBW) emission increases three-fold at L- to H-transitions as the edge density magnitude and gradient increase [7]. ELMs modulate the EBW emission. Gas puff imaging (GPI) [8] provides visual evidence of the barrier as it develops, and shows a concomitant decrease in edge turbulence. After the L–H transition, the H-mode phase can be sustained at a power less than the threshold power. H-modes have been obtained on NSTX only in lower-single null divertor (LSND) configurations, where the ion ∇B drift is towards the X-point, even though the centre stack limited (CSL) configuration is most common, with very limited operation in upper-single null divertor (USND) and double null divertor (DND) configurations. The ELM-free H-mode will be discussed in section 2 and ELMy H-modes in section 3. Results of a power threshold study is reported in section 4, and a summary is presented in section 5.

2. Time evolution of the NSTX ELM-free H-mode

Studies of the dynamics of the NSTX H-mode must include times significantly before the L- to H-mode transition since early heating and operational factors affect the transition, the characteristics of the resulting H-mode, and whether an ELMy or ELM-free H-mode results. As indicated earlier, H-modes have only been obtained in NSTX when a LSND is created. The operating range and parameters for NSTX H-modes are as follows: inner wall gap of >1–2 cm for the LSND, $840\,\mathrm{kW} < P_\mathrm{NBI} \leqslant 2.5\,\mathrm{MW}$, $B_\mathrm{t} = 0.45\,\mathrm{T}$ and $0.7\,\mathrm{MA} < I_\mathrm{p} < 1\,\mathrm{MA}$ for NBI-only H-modes. H-modes were obtained also with RF only heating with $0.40\,\mathrm{T} < B_\mathrm{t} < 0.45\,\mathrm{T}$ and $0.35\,\mathrm{MA} < I_\mathrm{p} < 0.5\,\mathrm{MA}$. In general, $\bar{\mathrm{n}}_\mathrm{e}$ was in the range $\sim(1.5\text{–}2.5 \times 10^{19}\,\mathrm{m^{-3}}$ at the L–H transition. The duration of H-modes on NSTX was in the range of 500 μs–130 ms. H-modes have not been obtained in plasmas that were heated only with Ohmic heating. Very often, when the LSND was created late in the discharge, the resulting H-mode was ELM free. An example of this can be seen in figure 1, which shows an overlay of operation and plasma parameters for an ELM-free H-mode and an L-mode plasma. These discharges were programmed identically, but the second one had an H-mode transition. The L-mode was run at the same I_p as the preceding discharge, and it was common that H-modes were accessed in NSTX on the second (and succeeding) of identically programmed discharges. This could be a wall conditioning effect.

The largest energy confinement time τ_E ($\sim$120 ms) observed so far for all discharges in NSTX occurred in the 0.90 MA discharge of figure 1 (as can be seen in figure 1(c)), for

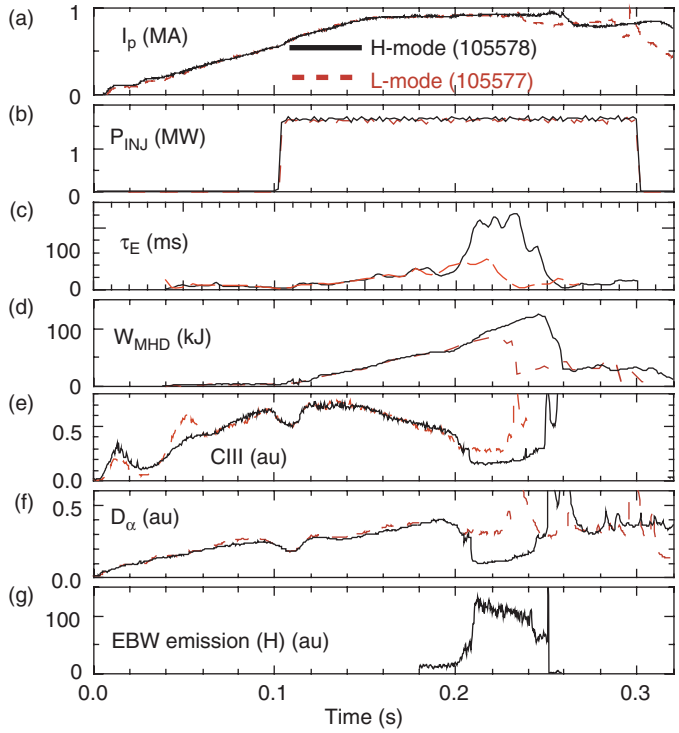

Figure 1. Time variation of operating and plasma parameters for an L-mode (- - - -) and an H-mode plasma (——). Shown are (*a*) plasma current I_p, (*b*) NBI power, (*c*) energy confinement time τ_E, (*d*) stored energy W_{MHD}, (*e*) CIII emission, (*f*) D_α emission, (*g*) EBW emission.

which the stored energy reached a peak value of ∼125 kJ (figure 1(*d*)). The stored energy was determined by magnetic measurements using EFIT [9]. The time rate of change of the total energy was accounted for in calculating the loss power; however, contributions by fast beam ions could not be determined at this time and this component was not subtracted from the stored energy. This τ_E is about a factor of 2 greater [1] than that predicted by a high β, ELM-free scaling obtained from an international H-mode database [10]. The plasma was diverted at 200 ms, 100 ms after NBI was turned on. The H-mode transition took place at ∼208 or 8 ms after the plasma was diverted. At the time the plasma is diverted, the visible light at the centre stack reduces dramatically. When the H-mode is obtained, the edge visible light is reduced, the D_α signal drops (figure 1(*g*)), and large amplitude fluctuations on a midplane centre stack Mirnov coil are reduced [1]. The reduction in edge light due to a reduction in neutral influx was an indicator of the formation of an edge transport barrier.

At the H-mode transition the n_e profile becomes strongly peaked at the edge, inside the magnetic separatrix ($R_{sep} \sim 1.5$ m), with a ear shaped pedestal (also observed on MAST [3]) which persists throughout the duration of the ELM-free phase (figure 3(*a*)). Figure 2 gives electron density and temperature (n_e and T_e) profiles for several different discharges as measured by Thomson scattering. n_e profiles are plotted in figure 2(*a*) for shot 105578 for time slices at $t = 0.195$, 0.212, 0.228 and 0.245 s, showing the time evolution of the n_e profile from just before the L–H transition to just before termination. Figure 2(*b*) shows T_e as well as ion temperature and toroidal velocity (T_i and V_ϕ) profiles for a time just before the L–H transition for a different shot, but which was similar to the shot of figure 1. Central

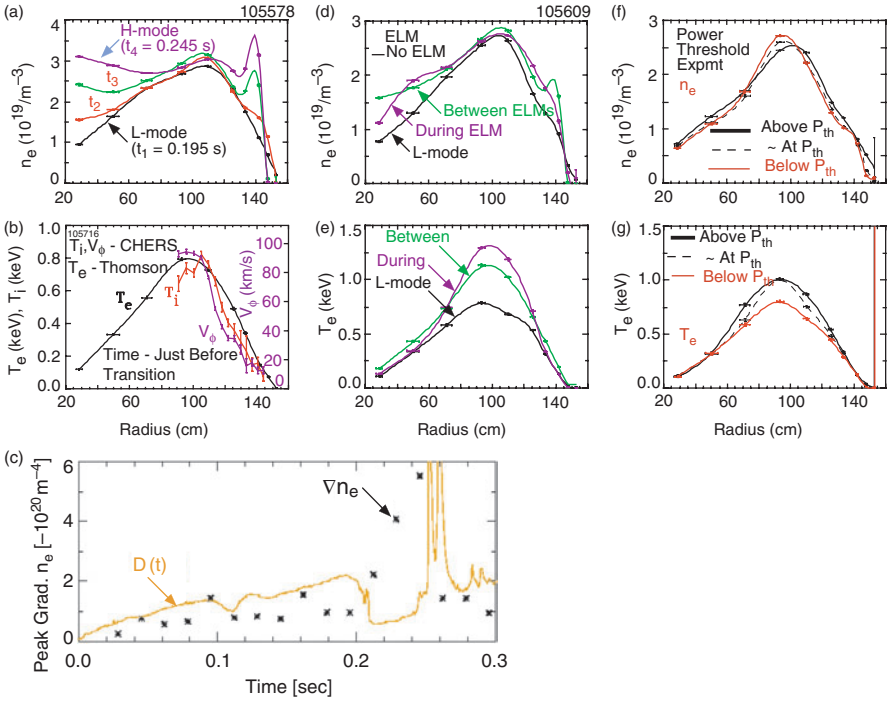

Figure 2. n_e and T_e profiles for several H-mode plasmas: (*a*) n_e profiles during evolution of the H-mode of figure 1 at $t_1 = 0.195$, $t_2 = 0.212$, $t_3 = 0.228$ and $t_4 = 0.245$ s, (*b*) T_e, T_i and n_e profiles for a time just before L–H transition, (*c*) D_α emission data and edge density gradient, dn/dr, from Thomson scattering measurement (*d*, *e*) n_e and T_e profiles for times just before L–H transition, during an ELM, and between ELMs for the discharge of figures 6(*d*)–(*f*), and (*f*, *g*) for three discharges of the P_{th} determination; NBI below, at, and above the threshold.

ion temperatures ($T_i(0)$) from a neutral particle analyser (NPA) were $T_i(0)_{NPA} \sim 740$ eV at $t \sim 180$ ms (about the same for $T_i(0)_{CHERS}$) just before the transition and $T_i(0)_{NPA} \sim 850$ eV at 20 ms into the H-mode, an increase of ~100 eV. The maximum edge n_e gradient observed in H-modes was $>6 \times 10^{20}$ m^{-4}. Figure 2(*c*) shows the time evolution of the peak dn_e/dr in the ELM-free H-mode of figure 1. The maximum value in this case was $\sim 5.7 \times 10^{20}$ m^{-4}. Figures 2(*d*) and (*e*) show profiles for an ELMy shot and figures 2(*f*) and (*g*) are profiles from three shots of a power threshold experiment.

Generally, in tokamaks the edge transport barrier affects the overall global confinement and transport, including the plasma core. There has been recent activity in the world fusion community to characterize the edge pedestal to test physics models and to be able to extrapolate to the next fusion device. The 'ears' on the n_e profile in ST ELM-free H-mode plasmas appear to be the norm and their implications relative to theory must be determined.

For the ELM-free H-mode of figure 1, the peak n_e increased to $\sim 3.5 \times 10^{19}$ m^{-3} at the time of the peak in the stored energy (~125 kJ at $t = 246$ ms) before the 'terminating event' at ~253 ms. The terminating event in ELMy H-modes (and L-modes) appears to be a locked mode, and this event should be delayed (in the next run) by reductions in the error magnetic field, due to coil modifications. The terminating event in ELM-free plasmas was often a growing island and sometimes an external kink. It is anticipated that improved machine conditioning with a new 350°C bake capability and improved current programming will delay or eliminate these terminations.

The emission from fundamental thermal EBW, mode-converted to the electromagnetic X-mode at the upper-hybrid resonance layer, increased by a factor of 3 at the H-mode transition [7]. This was a result of the sudden increase in the edge electron density gradient which increased the mode conversion efficiency. The increase in EBW signal is shown in figure 1(*g*). Very often, just before the transition, precursor oscillations in the main chamber D_α signal appear, which are also seen in the EBW emission. The oscillations are also seen in the D_α signal from a camera viewing the divertor plates.

The EBW signal remained elevated throughout the ELM-free phase; at the same time, the intensity of the D_α light remained reduced. The signal from the central viewing chord (not shown) of the bolometer array usually increased during ELM-free H-modes. The D_α profiles at the bottom divertor plates showed peaks near the strike points, as can be seen in figure 3. Just before the L–H transition for the ELM-free shot of figure 1, the peak emission for the outer divertor plate was much greater than that for the inner plate. However, in general during the L-mode phase, the particle flux can peak on either plate. After the transition, the inner divertor peak D_α emission became much larger than the outer and increased all during the ELM-free H-mode, increasing to six times its initial value just after the transition. Once the plasma transitioned into the H-mode, and during the initial ELM-free phase and between ELMs, the inner plate D_α was always higher. It is not known if this is an atomic physics effect (i.e. change in ionization/excitation rates), a shift of the in/out particle flux ratio, or a change in the poloidal profile of the cross-field flux feeding the scrape-off layer (SOL). Toward the end of the H-phase, as the D_α signal gradually increased, the EBW signal decreased. There was a fast increase in D_α at ∼0.242 s with a concomitant rapid drop in the EBW signal to a new plateau level before the H-phase was terminated at $t \sim 0.254$ s. $n = 1$ MHD mode activity was observed in the edge of the ELM free H-mode within the frequency range 50–80 kHz. In this case, the mode disappeared at $t \sim 0.2$ s, a few ms before the initial gradual rise in the EBW signal, and 8 ms before the major drop in D_α. The frequency of the mode remained fairly steady between 50 and 80 kHz up to the transition.

Changes in edge turbulence during H-mode operation were seen using a GPI diagnostic which views the He-I (587.6 nm) light emitted from an He gas puff within a radial/poloidal

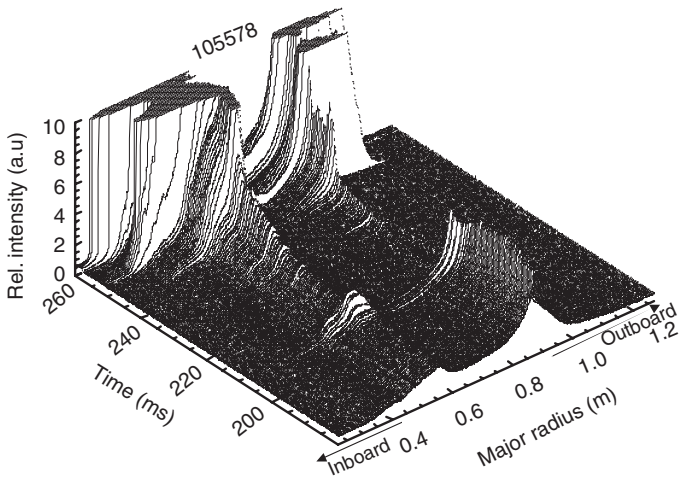

Figure 3. D_α emission from the lower divertor showing the peaks at the strike points on the inner and outer divertor plates. For this ELM-free H-mode, peak emission is on outer plates before transition and shifts to inner plate at L–H transition and during H-mode.

view near the outer midplane separatrix [8]. The fluctuations in He-I light emission are related to the edge density turbulence [11] and perhaps also to edge temperature fluctuations. GPI demonstrates very clearly the role of H-mode physics in the dynamic evolution of the edge plasma turbulence during L- to H-transitions and H- to L-transitions. The onset of H-modes in NSTX causes a sharp decrease in the radial width of the He-I emitting region (similar to that seen for naturally occurring D_α in other devices), as shown in figures 4(*a*)–(*c*). Since the He-I emission without an H-mode was strongly fluctuating in space and time, this sharpening may be attributed to a reduction in the edge turbulence level. The sharpening could also be related to the strong edge gradients during the H-phase. Examples of the time dependence of the He-I light emission during an L–H and an H–L transition are shown in figures 4(*d*)–(*g*), for a point within the sharp barrier region and a point exterior to it. The L–H transition occurred over a ≈1 ms timescale and there was usually one (or more) unusually large spike of He-I light emission at the instant the transition began. The transition from H- to L-mode occurred

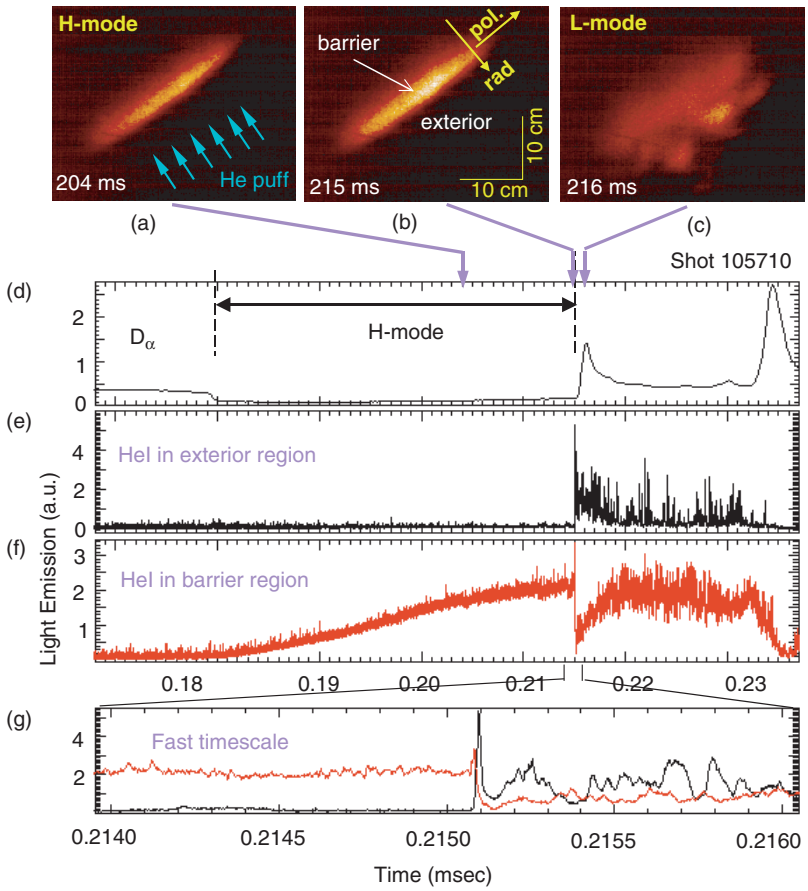

Figure 4. (*a*)–(*c*) Images of the edge of NSTX while an He gas puff is being injected into a 1.0 MA, 0.45 T discharge. While a quiescent, sharp edge is observed during H-mode, turbulent eddies and a diffuse edge are observed in L-mode. Each frame is exposed for 10 μs and registered in neutral helium emission at 587.6 nm. (*d*)–(*g*) Time series of light emission. The H- to L-transition occurs in ∼20 μs, comparable to the turbulence autocorrelation time. Arrows indicate times of images in figures 4(*a*)–(*c*) shown at the top of the figure.

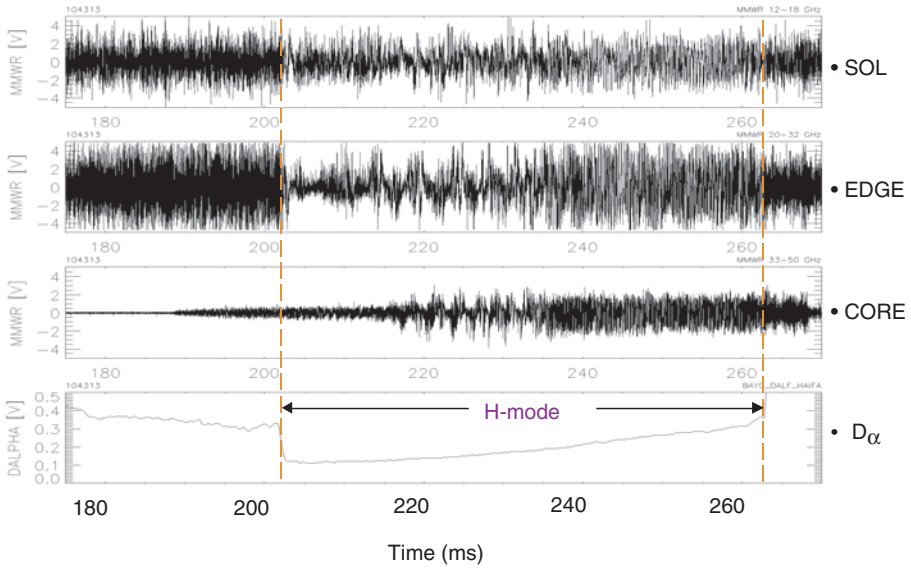

Figure 5. Edge reflectometer signals showing reduced turbulence in the plasma edge during the H-mode, while fluctuation levels in the SOL and core remain unchanged just after the L–H transition. The frequencies of the homodyne reflectometer are 15, 26 and 45 GHz, corresponding to cut-off densities of 3×10^{18} m^{-3} (SOL), 8×10^{18} m^{-3} (edge) and 2.5×10^{19} m^{-3} (core), respectively.

much more rapidly and without any apparent precursors. In many cases this H–L transition timescale was comparable to the edge turbulence autocorrelation time of 30–40 μs measured using this GPI system in other machines [11]. Detailed quantitative analysis of these signals and their interpretation in terms of edge turbulence and edge profile changes is in progress. Edge turbulence reduction was also observed using the edge scanning reflectometer. Figure 5 shows reflectometer signals for an ELM-free H-mode similar to shot #105578. At the L–H transition at ~200 ms, the edge turbulence (inside the separatrix) is reduced, but the SOL and core turbulence are unchanged. During the ELM-free phase, the edge and core turbulence levels actually increased back to and above pre-transition levels respectively, while the SOL was unaffected.

3. Evolution and characteristics of ELMy H-modes

ELMy plasmas were obtained for the first time when the formation of the LSND was moved to an earlier start time, 0.135 s compared to 0.20 s for the ELMy and ELM-free cases, respectively. ELMs were obtained under various conditions with both NBI heating and HHFW heating. The ELMy H-modes showed a rapid increase in the EBW signal at the instant of the transition (D_α drop), to the same level as in the ELM-free case (compare the EBW signals at the beginning of the H-mode in figures 1 and 6). Shown in figure 6 are the D_α, W_{MHD} and EBW signals for two plasmas with ELMs. In the first case there were what appeared to be large low-frequency compound ELMs, as are often observed near the L–H power threshold in conventional aspect ratio devices. In the second case is a plasma which exhibited the classic characteristics of a higher frequency, smaller amplitude, ELMy H-mode. However, with each large ELM, the EBW intensity decreased below the pre-transition level. This large perturbation on the EBW signal is consistent with the strong perturbations on the n_e and T_e profiles for the large ELM

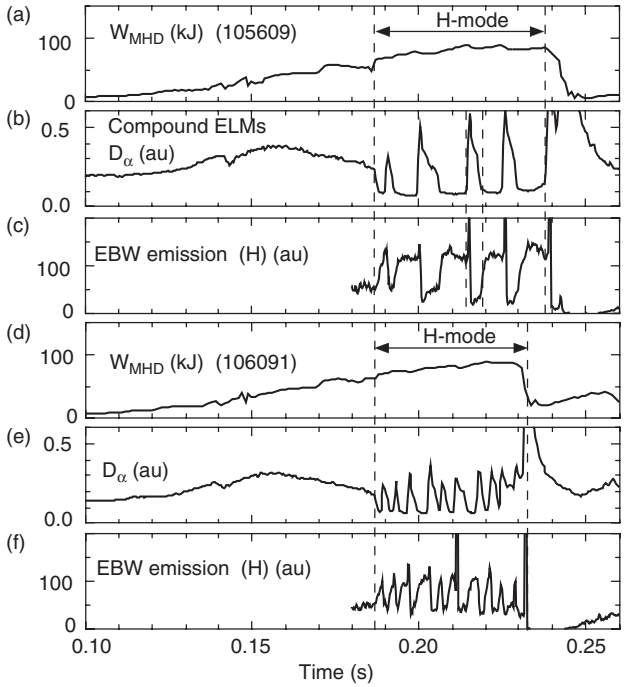

Figure 6. Time evolution of stored energy (W_{MHD}), D_α emission and emission from EBW for a large ELM H-mode (*a*)–(*c*) and for small higher frequency ELM H-mode (*d*)–(*f*). At $t \sim 80$ ms for both cases, 1.6 MW of NBI power are turned on.

case shown in figures 2(*d*) and (*e*), respectively. Figures 2(*d*) and (*e*) show profiles before the L–H transition, during an ELM, and between ELMs.

The apparent 'ears' on the n_e profile disappeared during ELMs and the edge T_e decreased back to the L-mode shape over a region which extends well into the core plasma. This is different from the more edge localized effect on the profiles usually observed in conventional tokamaks. For smaller and more frequent ELMs, the EBW signal decreased to about its pre-transition level as can be seen in figure 6(*f*). The large ELM behaviour of the EBW signal of figure 6(*c*) had an interesting structure, showing large spikes at the beginning of each ELM. The spike is considered [12] to be due to non-thermal emission. Similar non-thermal bursts were seen on ECE signals on TFTR [12] as measured using a grating polychromator viewing the edge of the plasma on the outboard (large major radius) side. For the small higher frequency ELMs, only one or two such spikes resulted. In contrast to the ELM-free H-mode of figure 1, both of the ELMy H-modes of figure 6 showed no peaking of radiative emissivity (however, the increase in core stored energy was also limited). The D_α signal (not shown) from the 1D lower divertor viewing CCD camera showed large emission spikes at each ELM. The ELM behaviour also varied with NBI power, as ELMs changed to dithering as P_b was reduced from 1.5 to 0.84 MW, i.e. at the power threshold. τ_E was ~50 ms for the ELMy H-mode of figures 6(*d*)–(*f*).

4. Power threshold and comparisons to models and conventional tokamaks

Understanding the L–H threshold physics would help in extrapolating to the next device with confidence. A dedicated power threshold experiment was conducted in order to examine the

changes in the plasma profiles leading up to the transition so as to compare with predictions from L–H transition theories. The experiment was carried out at fixed I_p and B_t of values ~900 kA and 4.5 kG, respectively. Only NBI heating was used and the power was varied from 0.7 to >1.6 MW. At 700 kW, the NBI power, P_b, was below the threshold. $P_b \sim 840$ kW was slightly above the threshold and dithers [13] were observed. At $P_b = 1.6$ MW the ELMs were large and 'normal'. This behaviour of the ELMs tending to be smaller and grassy and finally more like dithers as power is lowered toward the threshold value is also often observed in conventional aspect ratio tokamaks.

The plasma MHD activity, T_e, n_e, and other parameters were compared to determine if there were noticeable differences between the three power levels (below, at, and above threshold). n_e and T_e profiles for three shots of the threshold study are shown in figures 2(*f*) and (*g*), respectively. The profiles in each case are for times just before the transition. The thick curve is for a case well over the threshold, the dashed curve for the case at P_{th}, and the thin solid curve is for a plasma with heating power $< P_{th}$. It was found that the n_e and T_e profile shapes were similar for the three cases, as can be seen in figure 2. In general, no clear differences were seen for edge profile values for shots with and without H-mode transitions (i.e. comparison discharges).

The lowest power for H-mode access was ~840 kW (auxiliary heating power required above the Ohmic power, which was 1.15 MW). The ITER H-mode multimachine database scaling for the threshold power is $P_{th} = 0.65 n_e^{0.93} B_t^{0.86} R^{2.15}$ (MW, 10^{20} m^{-3}, T, m) [14], which, for NSTX yields 50–60 kW. It appears that the ITER scaling does not apply to STs. The ratio of observed lower limit to predicted threshold power is 33. When the dW/dt is folded in, the loss power is 1.1 MW, or 18 times the value given by the ITER scaling.

There are other power threshold scalings to which STs may be compared. For example, the ITER scaling has no I_p dependence, though for operational purposes, for TFTR, $P_{th}(\text{MW}) = 11 \times I_p$ (MA) was a reliable scaling for reproducibly obtaining H-modes [11]. The TFTR H-mode database was compared to that of ITER and it was found that $P_{th}(\text{TFTR}) \sim 2.72 \times P_{th}(\text{ITER})$. The TFTR database was dominated by supershot H-transitions. While an I_p dependence of the power threshold has not been quantified in NSTX, it is difficult to reliably trigger H-modes at $I_p \geqslant 900$ kA. Dnestrovskij *et al* [15] has recently introduced another threshold scaling for considering shots from START and T-10. The scaling is arrived at by using the full canonical profiles transport model (CPTM), which depends on local plasma edge parameters. The CPTM scaling is $P_{th}(\text{MW}) = 0.13(z_0 + z_q - z_n) R T_e(a) \kappa$ where $P_{tot} - P^{con} - P^{rad} > P_{th}$, $\kappa = n\chi = a^2 n / 2\tau_E$, $z_q = 3(1 - 1/q_a) \sim 2$–2.5, $z_n = -a n_a' / n_a$. Here, P^{con} is the power loss by conduction, P^{rad} is power loss by radiation, χ is the plasma thermal diffusivity, a is the minor radius, q_a is the edge stability factor, n_a is the edge density and n_a' is the edge density gradient. Initial application of this model to NSTX data yields a predicted power threshold just before the L–H transition between 100 and 500 kW, depending on the discharge. The present accuracy of the calculation is limited in NSTX by spatial resolution of the n_e and T_e profiles and also the uncertainty in the position of the separatrix. Other theories will be addressed in future H-mode studies and experiments on NSTX.

5. Summary and conclusions

In summary, L–H and H–L mode transitions have been obtained on NSTX using both RF and NBI heating. The H-modes have only been obtained in the LSND configuration; other configurations will require additional experimental studies and run-time. The H-mode threshold power using NBI alone was determined for a single combination of operational parameters, including $I_p = 0.9$ MA and $B_t = 0.45$ T, and found to be $P_{tot} \sim 2$ MW with a

P_b contribution of ∼840 kW. The best confinement time on NSTX to date is ∼120 ms, and this was obtained in an H-mode plasma. A maximum duration of the H-phase of ∼130 s has been realized in NSTX. Several diagnostic observations are consistent with existence of a strong edge transport barrier during the H-mode, including peaked edge density profiles and reduced amplitude of turbulent fluctuations. GPI shows very rapid return to L-mode during the H–L transition, within 20–30 μs. ELM-free and ELMy H-modes have been obtained; however, detailed characterization of the ELMs will be done in future experiments.

Acknowledgments

The authors thank the NSTX technical staff. This research was supported by the US Department of Energy under contracts DE-AC05-00OR22725, DE-AC02-76CH03073, W-7405-ENG-36 and grant DE-FG02-99ER54524.

References

[1] Maingi R, Bell M G, Bell R E, Bush C E and Fredrickson E O 2002 Characteristics of the first H-mode discharges in the National Spherical torus experiment *Phys. Rev. Lett.* **88** 035003
[2] Maingi R *et al* 2001 Characterization of H-mode discharges in NSTX *Proc. 28th EPS Meeting on Plasma Physics and Controlled Fusion (Madeira, Portugal, 18–22 June 2001)*
[3] Sykes A *et al* 2001 *Phys. Plasmas* **5** 2101
[4] Kaye S *et al* 1999 *Fusion Technol.* **36** 16
[5] Peng Y-K M 2000 *Phys. Plasmas* **7** 1681
[6] LeBlanc B P Private communication
[7] Taylor G , Egthimion P C, Jones B, LeBlanc B P and Maingi R 2002 *Phys. Plasmas* **9** 167
[8] Maqueda R J, Wurden G A, Zweben S, Roquemore L, Kugel H, Johnson D, Kaye S, Sabbagh S and Maingi R 2001 *Rev. Sci. Inst.* **72** 931
[9] Lao L L, St John H, Stombaugh R D, Kellman H G and Pfieffer W 1985 *Nucl. Fusion* **25** 1611
[10] ITER physics basis authors 1999 *Nucl. Fusion* **39** 2137
[11] Zweben S *et al Phys. Plasmas* at press
[12] Bush C E *et al* 1995 *Phys. Plasmas* **2** 2366
[13] ASDEX team 1989 *Nucl. Fusion* **29** 1959
[14] Snipes J A 1997 *Proc. 24th EPS Conf. (Berchtesgaden, Germany)* (Geneva: European Physical Society) Pt III, p 961
[15] Dnestrovskij Yu N *et al Proc. 26th EPS Conf. (Maastricht, the Netherlands)* p 178